University of Central Florida
STARS

Honors Undergraduate Theses | UCF Theses and Dissertations

2022

Design and Testing of a Hybrid Direct Ink Writing and Fused Deposition Modeling Multi-Process 3D Printer

Alexander X. Losada
University of Central Florida

 Part of the Computer-Aided Engineering and Design Commons
Find similar works at: https://stars.library.ucf.edu/honorstheses
University of Central Florida Libraries http://library.ucf.edu

This Open Access is brought to you for free and open access by the UCF Theses and Dissertations at STARS. It has been accepted for inclusion in Honors Undergraduate Theses by an authorized administrator of STARS. For more information, please contact STARS@ucf.edu.

Recommended Citation
Losada, Alexander X., "Design and Testing of a Hybrid Direct Ink Writing and Fused Deposition Modeling Multi-Process 3D Printer" (2022). *Honors Undergraduate Theses*. 1271.
https://stars.library.ucf.edu/honorstheses/1271

DESIGN AND TESTING OF A HYBRID DIRECT INK WRITING AND FUSED DEPOSITION MODELING MULTI-PROCESS 3D PRINTER

By

ALEXANDER LOSADA

A thesis submitted in partial fulfillment of the requirements
for the Honors in the Major Program in Mechanical Engineering
in the College of Engineering and Computer Science
and in the Burnett Honors College
at the University of Central Florida
Orlando, Florida

Fall Term
2022

Thesis Chair: Dazhong Wu, Ph.D.

Abstract

Multi-material 3D Printing allows the ability to fabricate parts with tuned mechanical properties, multi-process 3D printing widens the choices of available fabrication materials. The objective of this study is to build a custom 3D printing test bed that is capable of printing multi-material parts with fused deposition modeling and direct ink writing techniques. A 3D printer, controlled by an industrial motion control system, with FDM and DIW capabilities was built by combining FDM extruders with a pneumatic dispensing system on a single platform. By utilizing the Direct Ink Writing function, we expand the number of printable materials to include some off the shelf silicones and epoxies, as well as custom, user made, materials. This study will further expand the manufacturing and research capabilities within the additive manufacturing discipline.

Acknowledgements

Firstly, I would like to thank Dr. Dazhong Wu for inviting me to work with him in completing this project in his lab. Dr. Wu provided me with the freedom and space to solve the challenges associated with this project. The successful completion of this project could not have been realized without his guidance and encouragement.

Next, I would like to thank my father, Dan Losada who instilled in me, from a young age, work ethic, resolve, curiosity, and a willingness to learn from failure. Without his influence, I would have never been able to complete a project like this, let alone achieve any academic success.

Finally, I would like to thank my spouse, Natasha Lee, who, throughout my endeavor to earn my undergraduate degree, has sacrificed time spent with me, as well as provided financial and material support to our household.

Table of Contents

List of Figures

List of Tables

1. Introduction

Multi-material 3D printing is a technique by which different types of materials can be printed in a single part. A multi-material Fused Deposition Modeling (FDM) printer uses two or more extruders to print different thermoplastics in one part. Multi-process 3D printing is like multi-material 3D printing in that it too is a process for printing multiple materials in a single part. However, multi-process 3D printing allows a user to select materials that require different fabrication techniques. For instance, a thermoplastic could be printed along with a UV curing material, or a heat curing material, that starts out in a liquid state, and couldn't be printed with the FDM technique. This expands the number of available materials for 3D printing in one part.

Advances in multi-material 3D printing have allowed completed products to be 3D printed in one cycle. There are several commercial printers on the market that are capable of multi-material 3D printing, but they are all limited to a single process. Foremost among the challenges of multi-material 3D printing is material adhesion. In a typical multi-material 3D printer, parts are fabricated with the FDM technique. Materials available for printing with the FDM have different thermal properties, which can cause a lack of adhesion at the interface layer. In addition, any material to be printed in an FDM printer must be a thermoplastic, limiting the choice of materials. Direct Ink Writing (DIW) 3D printing is a type of extrusion based 3d printing technique, like FDM, but it prints with materials that start out in a liquid state, and are later cured, thereby allowing a wider range of material choice, including both off-the-shelf materials, and custom materials.

An FDM 3D printer fabricates parts made from thermoplastic. The thermoplastic is heated to a semi-molten state and then extruded through a nozzle along a pre-programmed path based on 3d geometry. Because the thermoplastic comes in a filament form, it must be driven by extruder mechanisms into the heater and nozzle. This means that the material is forced through the nozzle by the region of the material

that is un-melted, and since the stiffness of the un-melted material matches the stiffness of the melted and then re-solidified material, there is a limit to just how soft of a material one can print using the FDM method. In fact, a Bowden tube style extruder can, in some cases, struggle to print even common TPU. A direct drive extruder can do a better job at it, but still struggles at higher extrusion rates. But even a direct drive extruder cannot print the softest materials, and because FDM relies on melting it cannot print any material that is not a thermoplastic.

DIW can print a wide array of materials but requires that the materials be in liquid form during the printing process. It can print ceramics, epoxies, and silicones. Thus, it offers a wide range of material properties that can be printed. Furthermore, under the right printing conditions, DIW printing does not suffer from anisotropy to the same degree that FDM does. DIW also opens the possibility of printing with more commonly available, off the shelf, materials that are cheap and easy to obtain.

A multi-process 3d printer can offer the best of both FDM and DIW methods and open the possibility of entirely new printing techniques. Multi-process 3D printing has a different set of limitations than multi-material FDM printing. Most of these limitations come from the differing curing mechanisms of the materials being printed. A multi-process part may feature a thermoplastic printed alongside a heat-cured material, like a PLA/RTV combination. Another may feature a combination of thermoplastic with a UV-curing material. In the case of the thermoplastic and heat curing combination, the heating needs of the thermoplastic may prematurely cure the heat curing material, thereby reducing its adhesion properties. If an opaque material is printed alongside a UV curing material, it may block the UV light from reaching, and curing, the material.

There are few explorations into the possibilities of multi-process DIW/FDM printing. Certain common materials, like RTV silicone, widely used as an adhesive, have been successfully used to print simple structures.

The objective of this study will be to build a multi-process FDM/DIW printer. Tests will then be conducted to determine whether RTV silicone can be used to print more complex structures, and, because of its adhesive properties, be used to fabricate multi-process parts.

2. Literature Review

Many studies have been conducted on the direct ink writing process, but the actual extrusion process can be broken down into two principal categories: Screw-based extrusion, and syringe-based extrusion. Syringe based extrusion, which is pneumatic powered, can further be broken down into piston driven, and air driven extrusion. [1] In a study comparing screw-based extrusion versus syringe-based extrusion, it was found that the screw-based extrusion backflow the ink through the small gap between the screw and the extruder body. [1]

In a paper that studied the effect of rheological properties on direct ink writing, researchers found that the storage modulus plays an important role in the printability of 3D printing inks. An aluminum oxide ceramic gel was created, and then printed at various stages of an aging process. The longer the material was aged, the higher the storage modulus was in comparison to the loss modulus. When the ceramic gel was printed when the storage modulus was lower than the loss modulus, the ink was unable to hold its shape and move on to the curing process. However, once the storage modulus was higher than the loss modulus, parts could be successfully fabricated.[2]

The ability of DIW to print many different types of inks lends itself to a versatility not seen in FDM printing. Many studies have been conducted with many different types of inks, and many paths to successful part printing. Inks which utilize photocuring have been printed in a process called “Photocuring While Writing.” [3] Another group utilized a chemical curing process to successfully print free-standing structures made of a short carbon fiber reinforced thermoset ink that cured instantly at the extrusion nozzle tip. Their process involved arresting a chemical reaction in the extruder syringe by cooling the syringe to prevent the reaction from occurring until the ink was printed. [4] One research group was able to print multi-material soft robotics made of a liquid silicone rubber intended for casting. They achieved this by printing the silicone into a vat filled with a matrix gel that acted as a support structure during curing. The gel was then liquified, and the parts extracted. [5] Finally, a research group was able to print microfluidic devices made

of off-the-shelf RTV silicone, Dowsil 732. They utilized a syringe-based pneumatic dispensing system to achieve this, however, they did not explore printing parameter optimization, choosing instead to simply print at low pressure and low speed. [6]

3. Design and Testing

3.1 Test Bed

The 3D printing test bed will feature Aerotech linear stages to facilitate positioning. The Stages are equipped with NEMA 23 stepper motors capable of 20x microstepping for a maximum step count of 4000 steps per revolution. Coupled with 5mm pitch anti-backlash ball screws, the stages are capable of positioning accurately within $\pm 34 \mu m$, and have a resolution of $0.125 \mu m$. The FDM module will contain two direct drive extruders, and hot ends capable of heating to $280\ ^0C$. The DIW module will have a single syringe-based pneumatic extruder, with air pressure supplied by the Nordson Ultimus V adhesive dispensing system.

Motion control will be handled by Aerotech Ensemble MP controllers. All slicing will be done using Ultimaker Cura. The printer will be a fully functional multi-material 3D printer, with a heated bed.

3.2 Controller Communications

The Aerotech Ensemble MP control system is an industrial motion control and is not tailored to Computer Numerical Control (CNC) operation. An industrial motion control is typically set up for repeated tasks, sometimes requiring a user or system input. As such, the controller comes equipped with a significantly smaller memory size compared to a purpose-built CNC controller. Compounding this problem, the Ensemble controller is programmed via its own proprietary language, Aerobasic, and requires numerous peripheral files to be loaded into the controller. Additionally, the post processors used by Cura are not easily accessed or edited by end users.

A python script was written that converted Marlin flavor G-code to Aerobasic language, but it was found that, due to the memory limitations, only small parts could be printed.

Leveraging a feature in the Ensemble controllers that allows lines of code to be sent and executed by the controllers one by one, a python script was written that simultaneously manages the positioning,

thermal, and pneumatic subsystems of the printer. The script works by reading the previously converted G-code file line by line and communicating the instructions to the appropriate subsystems. Position and FDM extrusion commands are sent to the Ensemble controllers, temperature commands are sent to an Arduino programmed for PID control, and DIW extrusion commands are sent to the Ultimus V dispenser.

3.3 Pneumatic Dispenser Communications

The Nordson Ultimus V dispenser is intended to facilitate the precise application of liquid adhesives or other similar treatments by workers or robots on an assembly line. It features a programmable controller which can apply pressure and vacuum to a syringe loaded with the desired material. With no accessories, it is capable of applying up 100 psi of pressure, with a high-pressure adapter, it can reach an output of 700psi.

Programming can be done manually using buttons on the front of the dispenser, however, in the case of CNC use, it is better programmed via the unit's RS-232 port. To do this, the Ultimus V requires that instructions be transmitted in ASCII format, and be accompanied by an 8-bit checksum, based on the hexadecimal values of the transmitted characters. The first step is for the computer to ping the Ultimus with the "enquire" character. The Ultimus then responds with an "acknowledge" character. The program message can then be sent, and if the Ultimus accepts, it replies "A0." Finally, the computer sends an "End of Transmission" character. All of these actions must take place within 3 seconds from the time the "Enquiry" character was sent.

A script was written to allow a researcher in the lab to program the Ultimus V via simple prompts and input windows. This creates a simple, straightforward way for anyone to access the advanced features of the machine. The script opens a window with a dropdown menu, and the user selects the desired program parameter. Once the parameter is selected, a text box pops up with a prompt reminding the user of the correct input format. The user then types in the desired input and clicks the check button. The code is displayed for the user to inspect. The user may then send the code by clicking the send button. Clicking the

send button causes the script to compute the necessary character count and checksum values, and then transmit to the Ultimus system.

For automatic programming, part of the user programming script was grafted into the controller communications script. The appropriate CNC program commands cause the communication program to calculate the character count and checksum, the code is then immediately transmitted to the Ultimus for on-the-fly programming during CNC operation.

Initially, the dispense command was also transmitted via RS-232, but it was quickly discovered that this did not offer explicit control over the dispensing of material because the pressure and vacuum command used the same code. To remedy this the Aerotech control system was further modified with a solid-state relay to transmit a signal to the Ultimus dispenser's operator foot pedal input. This gives the CNC program explicit control over dispensing as a "pressure" command signals the Ultimus by closing the switch to the foot pedal input, and the "vacuum" command opens it. Repeated commands have no effect on the state of the switch.

3.4 Custom Cura Plugin

As previously discussed, Ultimaker Cura does not allow G-code post processors to be easily accessed or edited by end users. Much of the backend of Cura is written in C# and the files are buried deep within the program files. Fortunately, however, Cura allows users to write their own add-ins which can add functionality and modify the output of CNC code.

A custom add-in script was written for Cura that allows a user to make the appropriate settings for DIW operation, and outputs code that can be interpreted by the controller to operate the Ultimus dispenser. M10 and M11 were chosen as the output code for pressure and vacuum, respectively. The user selects the add in in Cura and is then prompted for pressure and vacuum values. Once the part is sliced and the G-code generated, the file will contain the codes to control the dispenser. M10 S## will set the pressure value, M11

S## will set the vacuum value. An M10 or and M11 by itself will simply turn pressure or vacuum on. This add-in eliminates the need for a user to manually modify the G-code to operate the Ultimus dispenser.

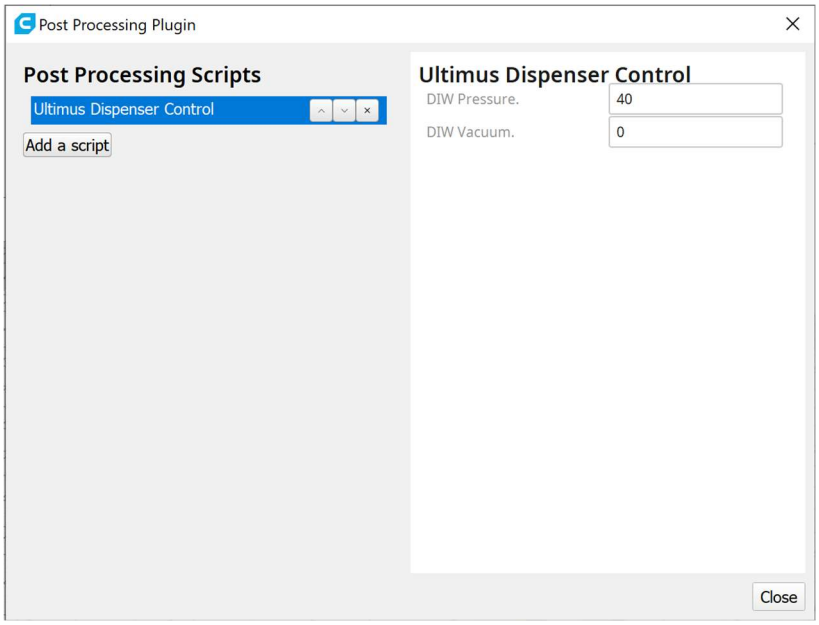

Figure 1: DIW Plugin Settings

3.5 3D Printing Test Bed Extruder Brackets

There are 3 standard syringe sizes for the DIW system, 3cc, 10cc, and 30cc. Each syringe has a different diameter. Additionally, each time a new print is started a new syringe must be loaded into the printer, as the material from the previous print is no longer useable. A quick-change bracket was designed that utilizes a V block to locate the syringe tip in the x direction, an interchangeable spacer to locate the syringe in the y direction, and finally, a spring-loaded clamp allows fast and easy positioning in the z direction. A syringe with fresh material can be loaded into the printer in under a minute.

The FDM bracket is a simple 3D printed bracket that holds two direct drive extruders and hot ends next to each other along the Y-axis.

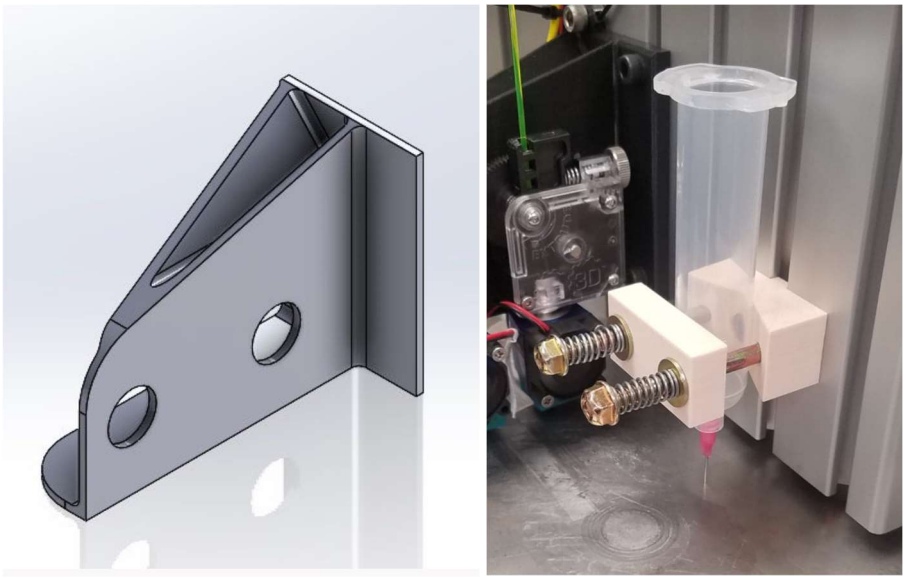

Figure 2: FDM Bracket (left) DIW Bracket (right)

3.6 Print Parameter Selection

The material selected for DIW printing was Dowsil 732. Dowsil 732 is a commonly available Room Temperature Vulcanizing (RTV) silicone. A python script was written to print a grid of lines with varying pressure on the Y-axis, and varying print speed on the X-axis. Pressure was varied from 50 psi to 90 psi and speed was varied from 2mm/s to 10mm/s. Nozzle sizes from 18 gauge to 25 gauge were tested. The lines were allowed to dry, and then the results were characterized by over-extrusion, optimal extrusion, and under-extrusion. Parameters that resulted in optimal extrusion were selected.

3.7 Single Material Beams

A set of single material beams was printed made of Dowsil 732 RTV silicone to ASTM-D790 [7] specifications. The print was repeated, further refining the parameter selection until a beam of acceptable quality was produced. All subsequent prints with Dowsil 732 were completed using the refined parameters.

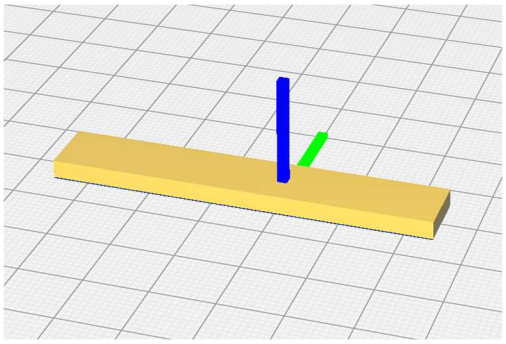

Figure 3: STL Model of Single Material Beam

3.8 Multi-Process Beams

A Multi-Process FDM/DIW beam was printed to ASTM-D790 specifications. It consisted of a PLA shell, with Dowsil 732 sandwiched in between. The PLA portions were printed at a temperature of 205 °C, and a speed of 50 mm/s. The Dowsil was printed with the parameters found from the single material beam printing tests. No further parameter refinement was performed.

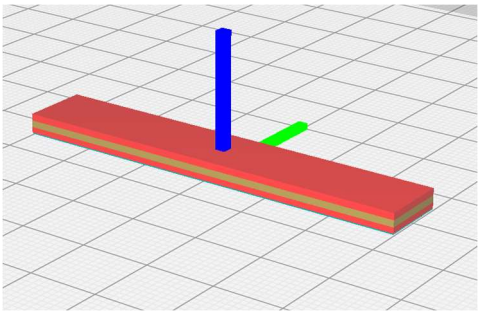

Figure 4: STL Model of Multi-Process Beam

3.9 Tensile Tests

Single Material RTV silicone tensile test specimens were printed to ASTM D638 specifications [8] using the DIW process. The specimens were then tested in a Shimadzu AGS-X universal test frame. Data was collected and analyzed.

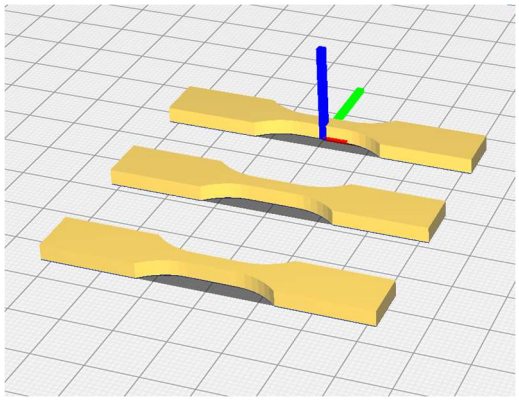

Figure 5: STL Model of Tensile Test Beams

3.10 Overhang Test

The “spiralize outer contour” setting in Cura was used to print vase structures of varying draft angles were printed made of RTV silicone by the DIW process. The wall thickness of the structures was 1 layer thick. The draft angles varied by 1 degree from 1 to 9 degrees, and then varied by 5 degrees from 10 to 20 degrees

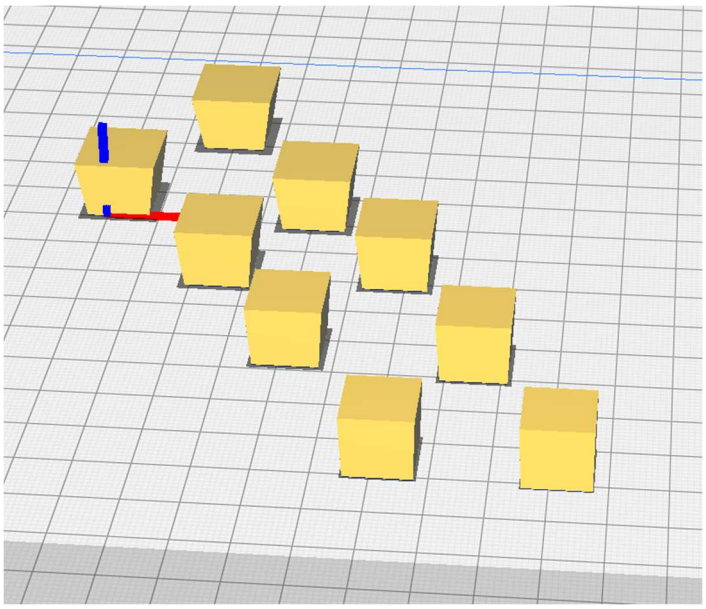

Figure 6: STL Model of 1-9 Degree Overhang Tests

3.11 Bridge Test

Sets of short towers were printed with varying distances between, and a “bridge” feature was printed between the towers. Distances varied by 5mm increments up to 20mm.

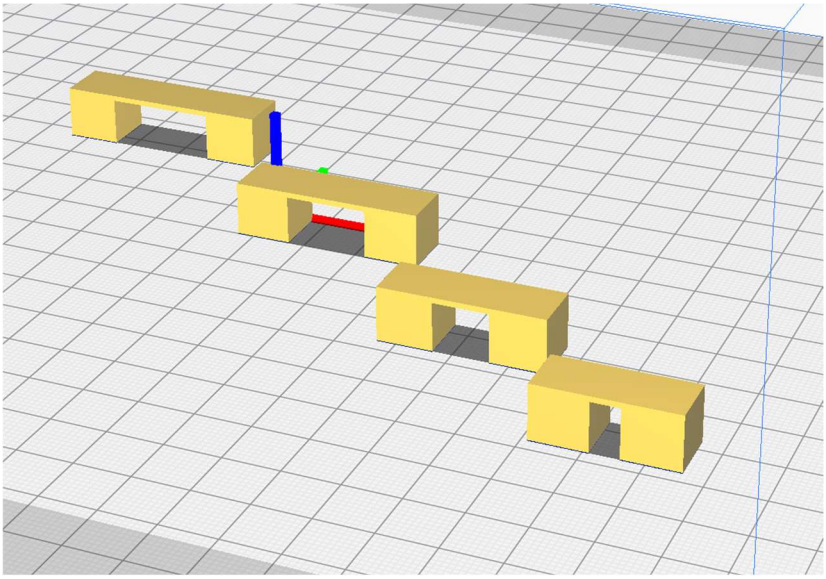

Figure 7: STL Model of Bridge Tests

4. Results

4.1 Print Parameters

The grid of printed lines was categorized into 3 types: under-extruded, over-extruded, and optimally extruded. An optimally extruded line has a uniform height, and nearly the same width as the diameter of the nozzle. An under-extruded line has a non-uniform height that peaks in the middle of the line, and a width smaller than the nozzle diameter. Over-extruded lines have a height larger than the printing layer height, with ridges on the sides of the line perpendicular to the printing direction, the width is also much larger than the nozzle diameter. Another type of defect that can be caused by user error when loading syringes is air bubbles, this defect manifests as an abrupt stop in extrusion with a semi-circle shaped under-extruded area in the middle of the line.

Figures 8 and 9 (below) show the grid and the defect types printed with gray RTV silicone, for visibility.

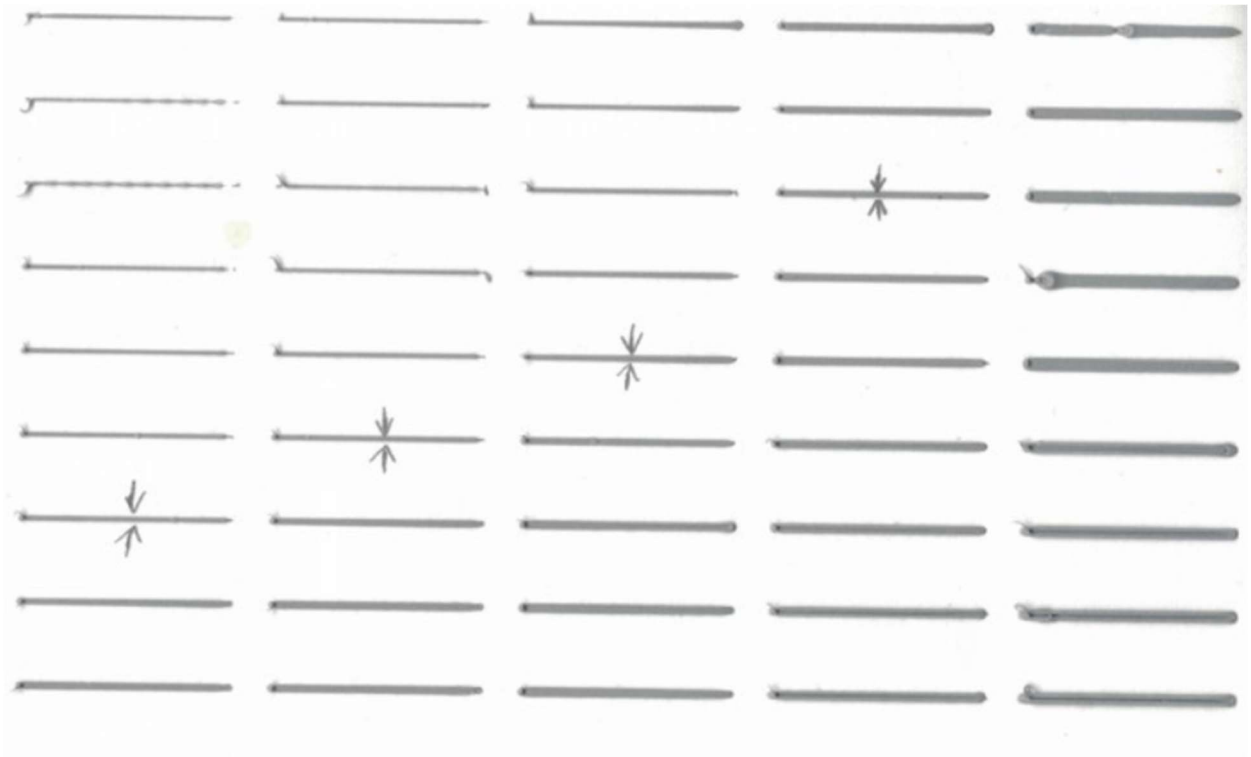

Figure 8: Scan of Printed Line Tests

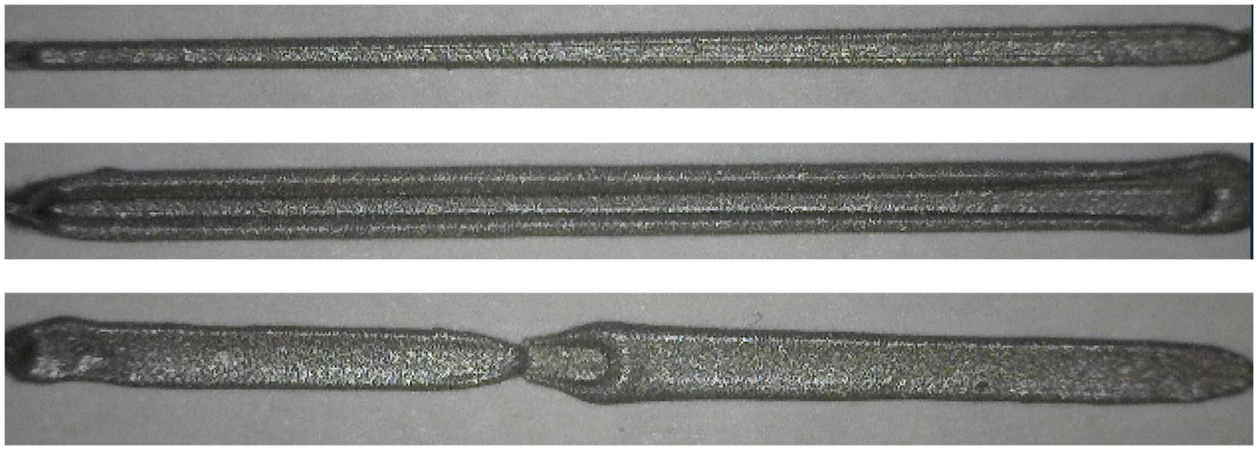

Figure 9: Closeup of Defect Types, Under extrusion (top), Over extrusion (middle), Air Bubble (bottom)

4.2 Single Material Print Quality

The single material beams (seen in figure) were categorized into 2 types: Over-extruded and optimally extruded. The over-extruded beams have blobs of material that appear near the corners and edges where the print head reverses during infill printing. The overall beam is also misshapen and layer lines are not visible. The optimally extruded beams have morphology that closely replicates the 3d model, with little to no extrusion defects. Layer lines are also visible on the side of the part.

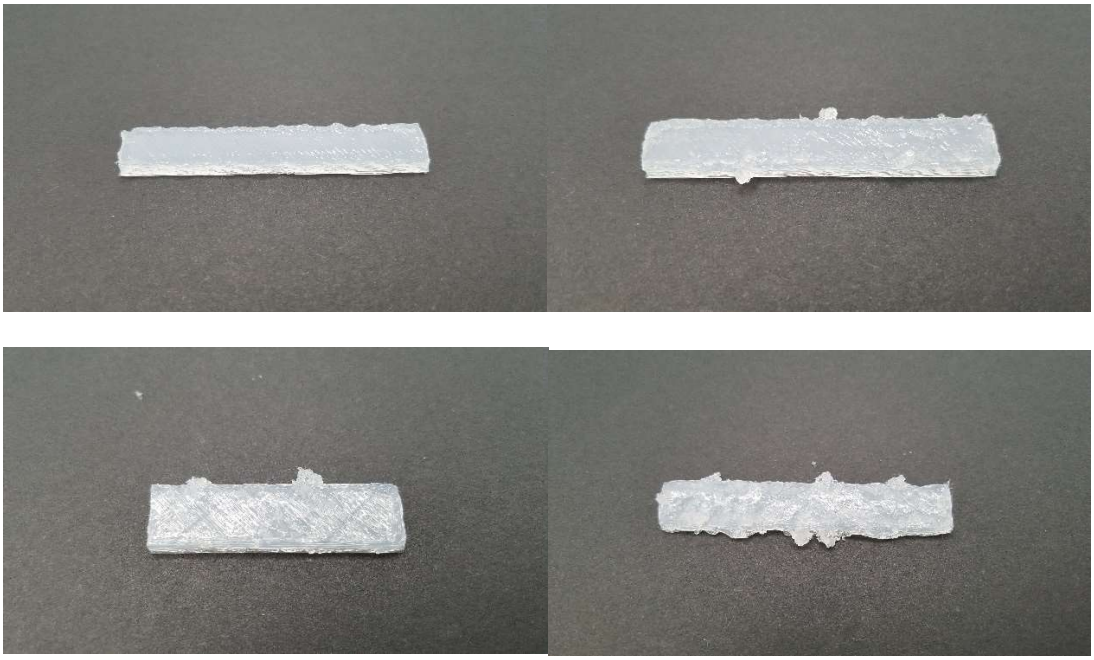

Figure 10: Single Material RTV Beams: 40 PSI, 10 mm/s (top left), 45 PSI, 10 mm/s (top right), 50 PSI, 10 mm/s (bottom left), 55 PSI, 10 mm/s (bottom right)

4.4 Tensile Strength

The tensile test samples were printed with the optimal printing parameters found in section 4.2. The finished tensile bars were of high quality and contained no air bubbles or any other imperfections. See figure 11 for print quality, and Table 1 for results.

Figure 11: Tensile Beam During Printing (left), Fully Cured Tensile Beam (right)

Tensile Strength testing revealed the following strength properties:

	Average	Standard deviation
Ultimate Tensile strength:	1.59 MPa	0.05 MPa
Young's Modulus:	0.25 MPa	0.05 MPa
Elongation at break:	613.46%	62.17%

Table 1: Tensile Strength Properties Dowsil 732 RTV Silicone

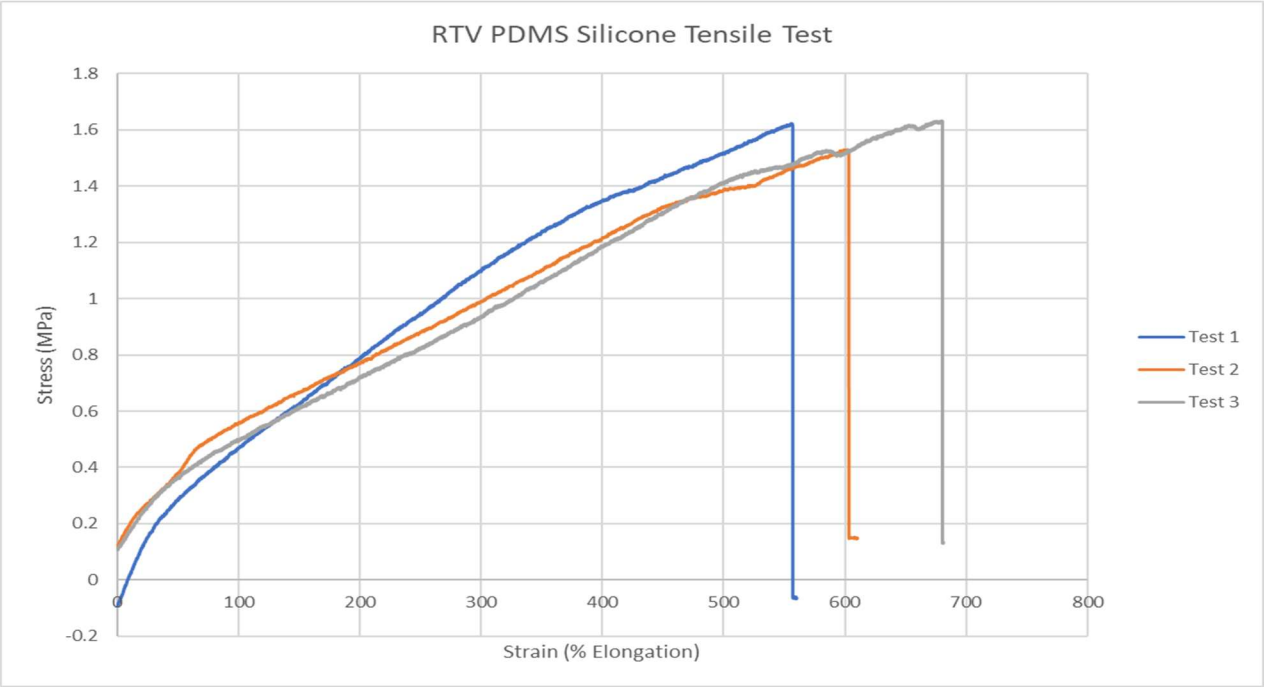

Figure 12: Graph of Stress/Strain Curve of Dowsil 732 RTV Silicone (3 identical samples)

Figure 13: Tensile Beam After Testing

4.5 Overhang Print Quality

In figure 14, it can be seen that none of the vase structures printed with good quality. However, it should be noted that the Spiralize Outer Contour setting in Cura only prints a single wall of the outer shape of the part, and during curing the structure relies on the strength of the RTV silicone that is still in a liquid gel state. Figure 14 shows the vase structures printed with various draft angles. Out of the parts with draft angles from 1 to 9 degrees, none completely failed, and the ones that are damaged are damaged from

interference with other parts of the printer. The 10-degree part turned out fairly good, like the lower draft angle parts, but higher draft angles lead to immediate print failure. No attempt was made to test the effect of increasing wall thickness, but we think that a structure printed with thicker walls may be more overhang tolerant.

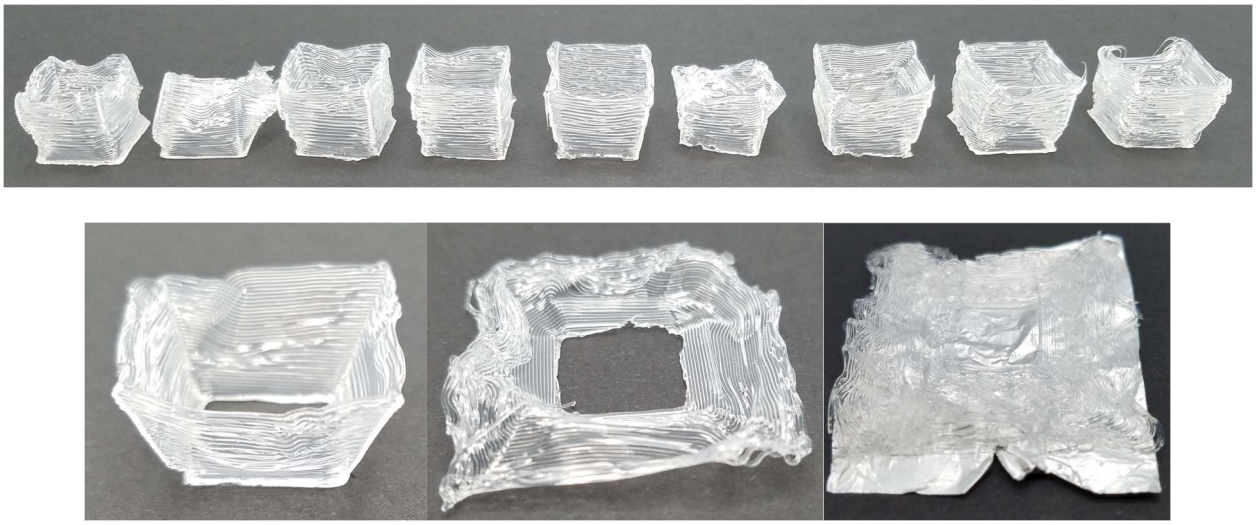

Figure 14: 1-9 Degree Overhang Tests (top row), 10-, 15-, and 20-Degree Overhang Tests (bottom row)

4.6 Bridge Print Quality

The Bridge Print test parts, like the overhang test parts, are not very good quality, and every bridge larger than 5mm failed immediately. Further refinements on parameter selection are need. Seen in the figure 15 (below), the bases of the bridge appear to be over-extruded, while the bridge itself is under-extruded. If the extrusion pressure was modified during printing to accommodate the needs of different sections of the part, this issue could be overcome. Further work is necessary.

Figure 15: 5mm Bridge Test

4.7 Multi-Process Beam

Figure 16 shows an initial attempt to print a multi-process, multi-material part. It consists of a PLA shell with RTV silicone in the middle. The test was of limited success because the curing of RTV is expedited by the addition of heat, and the print bed was heated to 60 C for printing the initial PLA layer. The heat caused the RTV silicone to rapidly cure as it exited the nozzle and begin to form blobs that were then pushed around by the DIW nozzle.

Figure 16: Multi-Process Beam

5. Conclusions and Future Work

5.1 Conclusion Summary

The addition of the DIW system to the test bed was a success. The programmable adhesive dispenser works in well in conjunction with the Aerotech industrial motion controller to deliver precise control over material extrusion. Preliminary testing shows that, given that a material has the right rheological properties, many materials are printable via the DIW method, including materials that are commonly available, like RTV Silicone.

Through printing parameter trials, the correct printing parameters were found for printing clear RTV silicone. Then, several parts were fabricated, including tensile test beams, rectangular beams, vase structures with various draft angles, and bridge structures with varying bridge distances. All tests showed promising results that suggest that, with further parameter refinement, many different types of structures can be successfully fabricated with the DIW method.

5.2 Future Work

As mentioned in section 3.1, the currently installed controller is inappropriate for a CNC application. Because of this, the test bed must be retrofitted with a CNC specific controller to continue being useful as more printing methods are added. The new controller should have expanded memory and be capable of extended trajectory planning to guarantee smooth, high-quality prints. In addition, the new controller should control all axes with a single main board, consolidating the control system into as few components as possible.

Multiple material DIW capabilities should be added to the test bed as well. This would allow combination prints of both hard and soft polymers and ceramics. Because parts printed by the DIW process can, under the right conditions, exhibit isotropic strength properties, DIW may be better suited for multi-material part fabrication. Further testing is needed.

Work has been conducted by other researchers to improve the print quality of DIW printed parts, this includes in-situ print monitoring that can adjust both path and extrusion parameters. [9] This work could be applied to the test bed and expanded on to produce fabricated parts of the highest quality possible.

The results of the initial multi-process show that further work is needed to produce a good sample. In the future, work will be done to refine the process parameters and increase the quality of multi-process FDM/DIW parts.

Appendix A: Bracket Parts

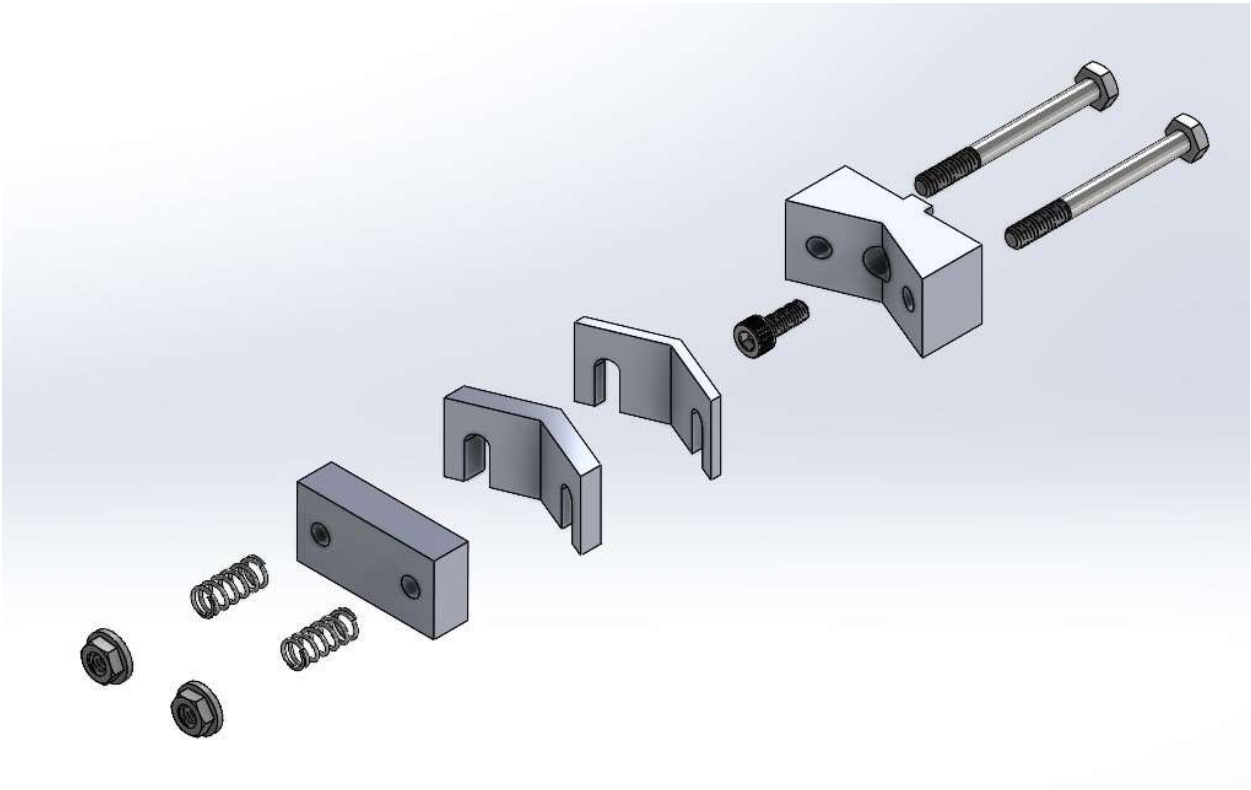

From bottom left to top right: Lock Nuts, Tension Springs, Clamp, 3cc Spacer, 10cc Spacer, Mounting Screw, V-Block, Guide Screws. The spacers are used to keep the center point of different size nozzles at the same location on the Y-axis.

References

[1] C.-F. Guo, M. Zhang, and B. Bhandari, "A comparative study between syringe-based and screw-based 3D food printers by computational simulation," *Computers and Electronics in Agriculture,* vol. 162, pp. 397-404, 2019, doi: 10.1016/j.compag.2019.04.032.

[2] A. M'Barki, L. Bocquet, and A. Stevenson, "Linking Rheology and Printability for Dense and Strong Ceramics by Direct Ink Writing," *Sci Rep,* vol. 7, no. 1, p. 6017, Jul 20 2017, doi: 10.1038/s41598-017-06115-0.

[3] J. Jin, H. Mao, and Y. Chen, "Photocuring-while-writing: A 3D printing strategy to build free space structure and freeform surface texture," *Manufacturing Letters,* vol. 29, pp. 113-116, 2021, doi: 10.1016/j.mfglet.2021.07.016.

[4] M. Ziaee, J. W. Johnson, and M. Yourdkhani, "3D Printing of Short-Carbon-Fiber-Reinforced Thermoset Polymer Composites via Frontal Polymerization," *ACS Appl Mater Interfaces,* vol. 14, no. 14, pp. 16694-16702, Apr 13 2022, doi: 10.1021/acsami.2c02076.

[5] Z. Wang, B. Zhang, W. Cui, and N. Zhou, "Freeform Fabrication of Pneumatic Soft Robots via Multi-Material Jointed Direct Ink Writing," *Macromolecular Materials and Engineering,* vol. 307, no. 4, 2022, doi: 10.1002/mame.202100813.

[6] Y. Jin, P. Xiong, T. Xu, and J. Wang, "Time-efficient fabrication method for 3D-printed microfluidic devices," *Sci Rep,* vol. 12, no. 1, p. 1233, Jan 24 2022, doi: 10.1038/s41598-022-05350-4.

[7] "Standard Test Methods for Flexural Properties of Unreinforced and Reinforced Plastics and Electrical Insulating Materials.pdf," doi: 10.1520/contact.

[8] "Standard Test Method For Tensile Properties of Plastic," doi: 10.1520/d0638-22.

[9] M. Piovarči *et al.*, "Closed-loop control of direct ink writing via reinforcement learning," *ACM Transactions on Graphics,* vol. 41, no. 4, pp. 1-10, 2022, doi: 10.1145/3528223.3530144.